OSEM Reconstruction, Associated with Temporal Fourier and Depth-Dependant Resolution Recovery Filtering, Enhances Results from Sestamibi and ^{201}Tl 16-Interval Gated SPECT

Pierre-Yves Marie, MD[1,2]; Wassila Djaballah, MD[1,3]; Philippe R. Franken, MD[4]; Chris Vanhove, PhD[4]; Marc A. Muller, MD[1]; Henri Boutley, Tc[1]; Sylvain Poussier, PhD[1]; Pierre Olivier, MD[1]; Gilles Karcher, MD[1]; and Alain Bertrand, MD[1,3]

[1]Department of Nuclear Medicine, University Hospital, Nancy, France; [2]UHP-INSERM U684, Nancy, France; [3]UHP-INSERM ERI13, Nancy, France; and [4]Department of Nuclear Medicine, Arizona-VUB, Brussels, Belgium

Gated SPECT recorded with 16 intervals determines left ventricular (LV) ejection fraction more accurately than does gated SPECT recorded with 8 intervals but produces higher image noise. This study aimed to assess the results from sestamibi and ^{201}Tl 16-interval gated SPECT when both signal-to-noise ratio and spatial resolution were enhanced with an original method of reconstruction. **Methods:** Forty patients with coronary artery disease underwent ^{201}Tl and sestamibi 16-interval gated SPECT and, to be used as a reference, cardiac MRI. Assessments of global and regional LV function provided by ordered-subsets expectation maximization (OSEM) with depth-dependant resolution recovery and temporal Fourier filtering were compared with those from conventional filtered backprojection (FBP) previously optimized by screening various filter frequencies and various temporal smoothing levels. **Results:** For both tracers, LV ejection fraction was determined best when the association of OSEM with depth-dependant resolution recovery was used alone, with temporal Fourier filtering, or with a slight 2-frame temporal smoothing: Mean absolute values of relative errors ranged from 3.2% to 3.6% (4.0%–7.9% for FBP), and coefficient correlation ranged from 0.91 to 0.93 (0.70–0.91 for FBP). Among these 3 reconstruction methods, the association of OSEM with depth-dependant resolution recovery with temporal Fourier filtering provided the highest signal-to-noise ratio, with mean increases of 54% for sestamibi and 80% for ^{201}Tl when compared with FBP, and the best analysis of segmental contractility, with exact agreement rates with MRI being 73% for ^{201}Tl and 79% for sestamibi. **Conclusion:** OSEM associated with temporal Fourier filtering and depth-dependant resolution recovery filtering enhances the LV function assessment provided by sestamibi and ^{201}Tl 16-interval gated SPECT and dramatically reduces image noise, a property that enhances and facilitates image interpretation.

Key Words: gated SPECT; MRI; ejection fraction; sestamibi; ^{201}Tl

J Nucl Med 2005; 46:1789–1795

Gated SPECT recorded with 16 intervals determines left ventricular (LV) ejection fraction more accurately than does gated SPECT recorded with 8 intervals but produces higher image noise (*1,2*). Image quality might, however, be enhanced by an ordered-subsets expectation maximization (OSEM)–based method of reconstruction, without significant loss of image resolution. The OSEM iterative method has better noise properties than does conventional filtered backprojection (FBP) (*3,4*) and dramatically reduces noise when combined with temporal Fourier filtering (*5*). In addition, results from OSEM reconstructions are improved when spatial resolution is enhanced by a depth-dependant resolution recovery prefilter (*6*).

This study aimed to determine whether the association of OSEM with depth-dependant resolution recovery prefiltering and temporal Fourier filtering, which is likely to improve both signal-to-noise ratio and spatial resolution, further enhances the results provided by ^{201}Tl and sestamibi 16-interval gated SPECT. Cardiac MRI was the reference method, and a comparison was planned with a conventional FBP method previously optimized by screening various filter frequencies and various temporal smoothing levels.

MATERIALS AND METHODS

We included 40 consecutive patients with coronary artery disease who were referred to our department for stress ^{201}Tl-SPECT with rest-reinjection; had a history of LV dysfunction, Q-wave myocardial infarction, or both; had a regular cardiac sinus rhythm; and gave written informed consent to participate. Sestamibi rest SPECT was always scheduled for just after the ^{201}Tl rest-reinjection acquisition, and cardiac MRI was scheduled for 1–10 d later.

^{201}Tl and Sestamibi Gated SPECT

Gated SPECT Acquisitions. As already described (*7–9*), 1.5 MBq of ^{201}Tl per kilogram of body weight were injected during

Received Apr. 29, 2005; revision accepted Jul. 15, 2005.

For correspondence or reprints contact: Pierre-Yves Marie, MD, Service de Médecine Nucléaire, CHU-Nancy, Hôpital de Brabois, 54511 Vandoeuvre Cedex, France.

E-mail: py.marie@chu-nancy.fr

exercise, and 0.5 MBq was injected 10 min before rest-reinjection imaging. Acquisitions were obtained on a double-head camera (DST-XL; SMV-GE Healthcare) equipped with high-resolution parallel-hole collimators, 32 projections being recorded on a 180° circular orbit from the 45° left posterior oblique to the 45° right anterior oblique orientations. Additional parameters were as follows: 16 bins, 50 s per projection, 50% acceptance window on the averaged length of cardiac cycles, 1.33 zoom, 43 × 43 cm field of view, 64 × 64 matrix, and a dual-energy window (60–90 and 150–184 keV).

When ^{201}Tl acquisitions had been completed, 11 MBq per kilogram of body weight of ^{99m}Tc-sestamibi were injected at rest, and an additional gated SPECT acquisition was started 50–60 min later using the same parameters except for energy window (126–154 keV) and time per projection (30 s).

Gated SPECT Reconstructions. For each of the 2 tracers, 25 different methods of reconstruction were analyzed (Fig. 1), including FBP and Butterworth prefilters with an order of 5 and various cutoff frequencies (0.20, 0.25, 0.30, 0.35, and 0.40 cycles per pixel) (*10*), and a depth-dependant resolution recovery prefilter followed by OSEM reconstruction with 2 iterations and 8 subsets (*6*). All these reconstructions were also obtained after an additional 2-, 3-, or 4-frame temporal smoothing of raw projections, each of the 16 bins from each projection being averaged with, respectively, the 1, 2, or 3 following bins. Finally, OSEM and depth-dependant resolution recovery prefiltering were also combined with temporal Fourier filtering applied after each iteration (*5*). Reconstruction time was around 1 min longer for depth-dependant resolution recovery with temporal Fourier filtering, when compared with FBP.

The depth-dependant resolution recovery filter (RESTORE; GE Healthcare) works on backprojected transaxial slices and involves, first, a Butterworth roll-off applied at intermediate to high frequencies for lowering image noise and, second, an inverse of the modulation transfer function applied at low to intermediate frequencies for correcting depth-dependant blurring (*6,11–13*). This inverse filtering varies according to the source-to-detector distance for each row of transaxial slices and is adapted to detector resolution (hole diameter, collimator length, intrinsic resolution). Forward projections were obtained before OSEM reconstruction.

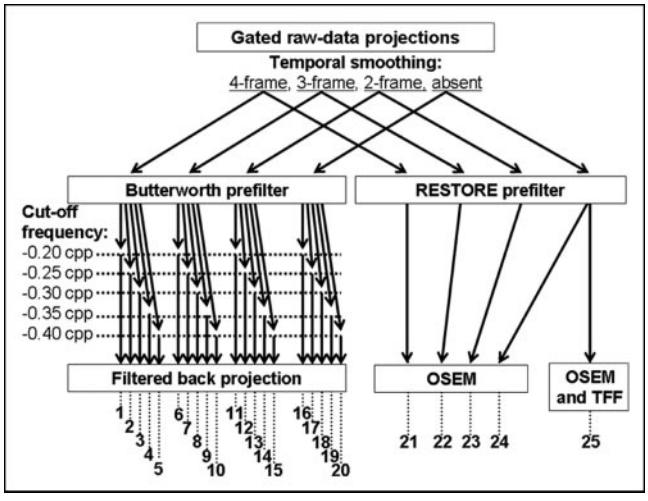

FIGURE 1. Schematic representation of 25 different methods used for reconstructing ^{201}Tl and sestamibi gated SPECT. Cutoff frequencies of Butterworth prefilters are expressed in cycles per pixel (cpp). TFF = temporal Fourier filtering.

Temporal Fourier filtering was applied to a Fourier series transform of the time–activity curves of the voxels and involves the suppression of all harmonics higher than the second one (those with a higher noise level) followed by an inverse Fourier transform (*5,14*).

Gated SPECT Analyses. LV volume and ejection fraction were determined automatically using Quantitative Gated SPECT software (Cedars-Sinai Medical Center (*1,15*)), constrained limits of contour detection being applied only in case of evident errors with the fully automatic process. Regional contractility was assessed visually by an experienced observer with a 17-segment LV division (*16*), the 2 proximal septal segments being excluded. According to wall motion and to the systolic increase in myocardial count, each segment was classified as akinetic/dyskinetic, hypokinetic, or normal.

To estimate signal-to-noise ratio, we selected a midventricular end-diastolic short-axis slice on each reconstruction. Mean myocardial counts (M_{My}) and corresponding SD (SD_{My}) were determined on a ring-shaped myocardial region of interest. Mean noise counts (M_{No}) and corresponding SD (SD_{No}) were determined on a half-moon–shaped region of interest, close to the left side of the lateral wall. Signal-to-noise ratio was estimated with the following formula: $(M_{My} - M_{No})/\sqrt{[SD_{My}]^2 + [SD_{No}]^2}$.

Acquisition and Analysis of Cardiac MRI

A breath-holding electrocardiography-triggered gradient-echo sequence (*17,18*) was used on a 1.5-T magnet (Infinity; GE Healthcare), with a phased-array surface coil and the following parameters: 8-mm slice thickness, 45-ms image frame duration, 30 × 30 cm field of view, and 256 × 128 matrix. Contiguous short-axis planes covering the entire LV volume were recorded, along with midventricular horizontal and horizontal slices. End-diastolic and end-systolic LV volumes, as well as LV ejection fraction, were measured on the contiguous short-axis planes using mass analysis software (Leiden University and MEDIS Medical Imaging Systems). Regional contractility was assessed visually by an experienced observer, according to the systolic increase in myocardial thickness and to wall motion and by using the same LV division and segment classification (1, akinetic or dyskinetic; 2, hypokinetic; 3, normal) as was used for gated SPECT.

Statistical Analysis

Continuous variables were expressed as mean ± SD. In a first step, the LV ejection fractions and end-diastolic volumes provided by each method of gated SPECT reconstruction and by each tracer were compared with corresponding MRI values by using linear regression analyses and paired comparisons of absolute values of relative errors (Wilcoxon tests). Relative error was computed as difference divided by mean of gated SPECT and MRI values.

In a second step, reconstruction methods providing the best determinations of LV ejection fraction and volume were selected for multiple paired comparisons of signal-to-noise ratio (Wilcoxon tests) and of exact agreement rates in segmental contractility analysis (McNemar tests). An exact agreement between gated SPECT and MRI required that the 2 techniques provide a similar contractility classification for a given segment but also that the quality of gated SPECT images be high enough for visual analysis of contractility. Contractility analyses were also assessed by determining the κ-values provided by visually analyzable recon-

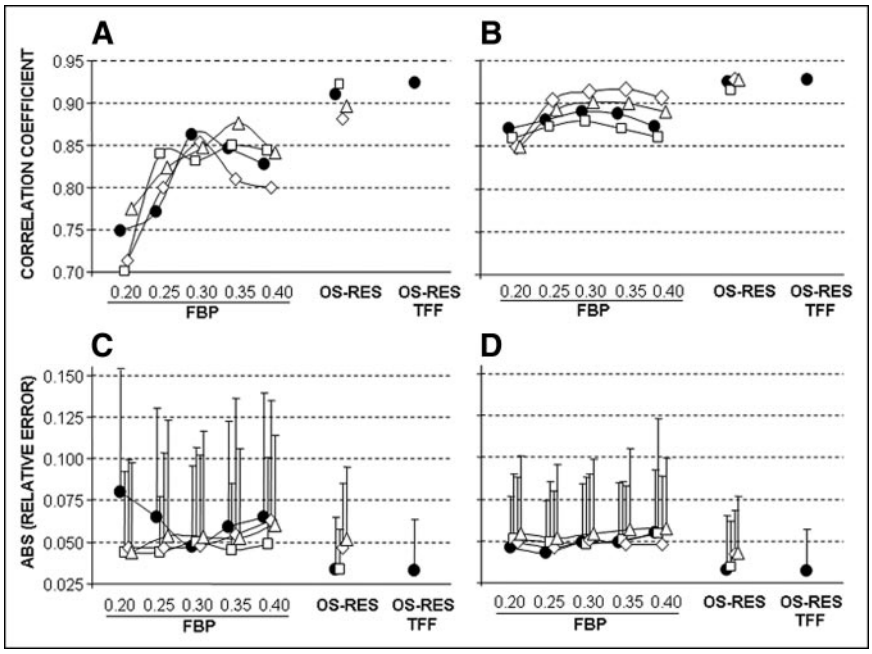

FIGURE 2. Correlation coefficients (A and B) and mean (±SD) of absolute values of relative errors (C and D) for LV ejection fractions determined with gated SPECT, reference values being provided by MRI. Gated SPECT with ^{201}Tl (A and C) or sestamibi (B and D) are reconstructed with FBP and various cutoff frequencies of Butterworth prefiltering (0.20, 0.25, 0.30, 0.35, and 0.40); OSEM with depth-dependant resolution recovery prefiltering (OS-RES); additional 2-frame (□), 3-frame (◇), or 4-frame (△) temporal smoothing or no temporal smoothing (●); and temporal Fourier filtering (TFF) associated with depth-dependant resolution recovery reconstruction.

structed gated SPECT. A P value of <0.05 was considered statistically significant.

RESULTS

Forty CAD patients were included: 80% were men, 85% had a history of myocardial infarction, and 80% had a Q-wave on electrocardiography. Mean patient age was 58 ± 11 y. At MRI, LV ejection fraction ranged from 16% to 70% and was lower than 40% in 21 patients (52%); 209 segments (35%) were akinetic or dyskinetic, 126 (21%) were hypokinetic, and 265 (44%) had normal contractility. At gated SPECT, mean myocardial counts per interval frame were 650,000 (±280,000) for sestamibi and 220,000 (±60,000) for ^{201}Tl ($P < 0.001$ compared with sestamibi).

Determinations of LV Ejection Fraction and Volume

On the FBP reconstructions provided by both tracers, the cutoff frequency of the Butterworth prefilter, but not temporal smoothing, had a clear impact on the quantifications of LV ejection fraction (Fig. 2) and volume (Fig. 3). For sestamibi, the best results were achieved at a cutoff of at least 0.30 cycles per pixel, whatever the level of temporal

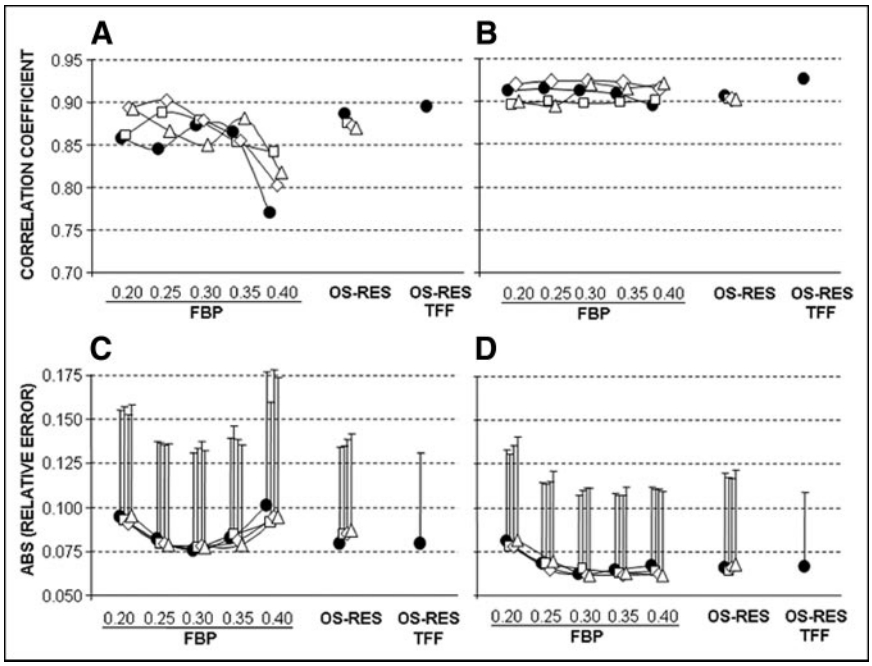

FIGURE 3. Correlation coefficients (A and B) and mean (±SD) of absolute values of relative errors (C and D) for LV end-diastolic volumes determined with gated SPECT, reference values being provided by MRI. Gated SPECT with ^{201}Tl (A and C) or sestamibi (B and D) are reconstructed with FBP and various cutoff frequencies of Butterworth prefiltering (0.20, 0.25, 0.30, 0.35, and 0.40); OSEM with depth-dependant resolution recovery prefiltering (OS-RES); additional 2-frame (□), 3-frame (◇), or 4-frame (△) temporal smoothing or no temporal smoothing (●); and temporal Fourier filtering (TFF) associated with depth-dependant resolution recovery reconstruction.

smoothing. Lower frequencies were associated with significant increases in the relative error for volume determination (Fig. 3). For ^{201}Tl, the best results were achieved at a cutoff of around 0.30 cycles per pixel. Lower or higher frequencies were associated with a decrease in correlation coefficient or with an increase in relative error for ejection fraction (Fig. 2), end-diastolic volume (Fig. 3), or both. Finally, whatever the considered tracer, 0.30 cycles per pixel was the lower cutoff frequency and, thus, the cutoff frequency leading to the higher image quality among those providing the best FBP determinations of LV ejection fraction and volume.

However, LV ejection fraction was better determined for both tracers when depth-dependant resolution recovery was used alone, with temporal Fourier filtering, or with only a slight 2-frame temporal smoothing: Correlation coefficients ranged from 0.91 to 0.93 and were higher than those documented with FBP (0.70–0.91), and mean absolute values of relative errors ranged from 3.2% to 3.6% and were always significantly lower than those from FBP (4.0%–7.9%) (Fig. 2). Compared with these 3 methods involving OSEM with depth-dependant resolution recovery prefiltering, higher relative errors were observed when strong 3- or 4-frame temporal smoothing was associated with depth-dependant resolution recovery reconstruction (Fig. 2), although differences were significant for ^{201}Tl ($P < 0.05$ for all comparisons) but not for sestamibi (P values ranging from 0.05 to 0.15).

LV volumes were lower than those from MRI, whatever the reconstruction method (all $P < 0.001$), and these volumes were not better determined with depth-dependant resolution recovery than with an optimal FBP (Butterworth filter of 0.30 cycles per pixel) (Fig. 3).

Compared with ^{201}Tl, sestamibi provided higher correlation coefficients and lower relative errors in LV volume determination whatever the method of reconstruction. For LV ejection fraction, results from the 2 tracers were more comparable, even though sestamibi provided higher correlation coefficients in most FBP reconstructions.

Signal-to-Noise Ratio and Regional Contractility Analysis

Factors involved in the visual analysis of gated SPECT images were compared between a reference FBP reconstruction (filter frequency, 0.30 cycle per pixel, no temporal smoothing) and the 3 reconstruction methods providing the best determinations of LV ejection fraction: the association of OSEM with depth-dependant resolution recovery prefiltering when used alone or with the addition of either 2-frame temporal smoothing or temporal Fourier filtering.

As detailed in Figure 4, whatever the considered tracer, gradual increases in signal-to-noise ratio were documented between FBP and the association of OSEM with depth-dependant resolution recovery prefiltering and temporal Fourier filtering. In addition, the increases in signal-to-noise ratios that were observed between these 2 reconstruction methods were clearly higher for ^{201}Tl (+80% ± 46%) than for sestamibi (+54% ± 40%, $P < 0.001$). Finally, whatever the method of SPECT reconstruction, signal-to-noise ratio was always significantly higher with sestamibi than with ^{201}Tl.

On FBP reconstructions, image quality was judged inadequate for the visual analysis of contractility in as many as 40% of patients for ^{201}Tl and in only 8% for sestamibi ($P = 0.03$), but all acquisitions from both tracers could be analyzed on each of the 3 reconstruction methods involving OSEM with depth-dependant resolution recovery prefiltering.

Results of segmental contractility analysis are detailed in Figure 5. The association of OSEM with depth-dependant resolution recovery prefiltering and temporal Fourier filtering provided the higher κ-values (sestamibi, 0.68; ^{201}Tl, 0.59), and the higher exact agreement rates (sestamibi, 79%; ^{201}Tl, 73%), and these rates were significantly better than those provided by the 3 other reconstruction methods. In addition, whatever the method of SPECT reconstruction, κ-values and exact agreement rates were higher with sestamibi than with ^{201}Tl. As illustrated by an example in Figure 6, the association of OSEM with depth-dependant resolution recovery prefiltering and temporal Fourier filtering consistently enhanced image quality and facilitated visual interpretation of gated SPECT images.

DISCUSSION

In the present study, 2 gated SPECT acquisitions were recorded consecutively at rest with ^{201}Tl and sestamibi using

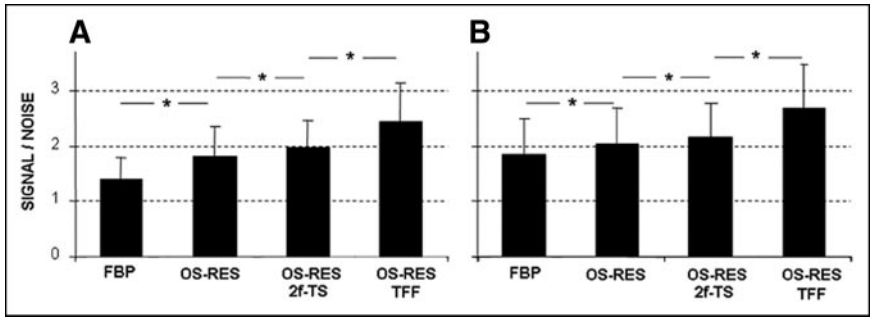

FIGURE 4. Mean (±SD) of signal-to-noise ratio index provided by ^{201}Tl (A) and sestamibi (B) gated SPECT on reference FBP reconstruction (filter frequency, 0.30 cycles per pixel, with no temporal smoothing) and on reconstructions providing best determinations of LV ejection fraction: OSEM with depth-dependant resolution recovery prefiltering (OS-RES), OS-RES with 2-frame temporal smoothing (2f-TS), and OS-RES with temporal Fourier filtering (TFF). *$P < 0.05$ for paired comparisons.

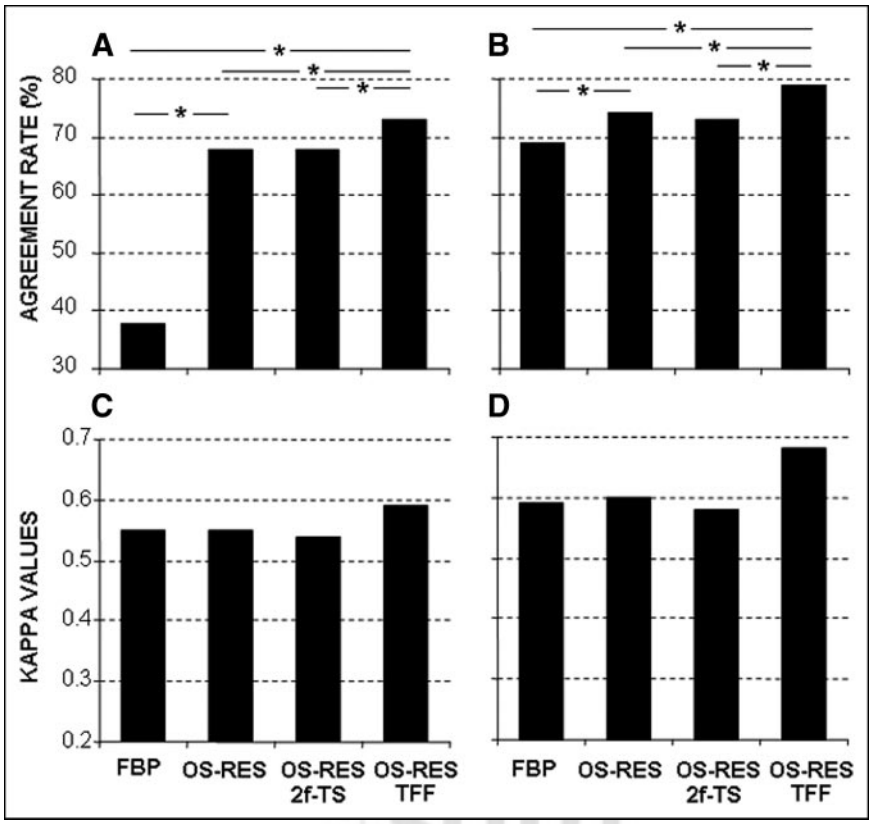

FIGURE 5. Exact agreement rates (A and B) and κ-values (C and D) with regard to MRI results for segmental contractility analyzed on ^{201}Tl (A and C) or sestamibi (B and D) gated SPECT and by using reference FBP reconstruction (filter frequency, 0.30 cycles per pixel, with no temporal smoothing) and reconstructions providing best determinations of LV ejection fraction: OSEM with depth-dependant resolution recovery prefiltering (OS-RES), OS-RES with 2-frame temporal smoothing (2f-TS), and OS-RES with temporal Fourier filtering (TFF). *$P < 0.05$ for paired comparisons.

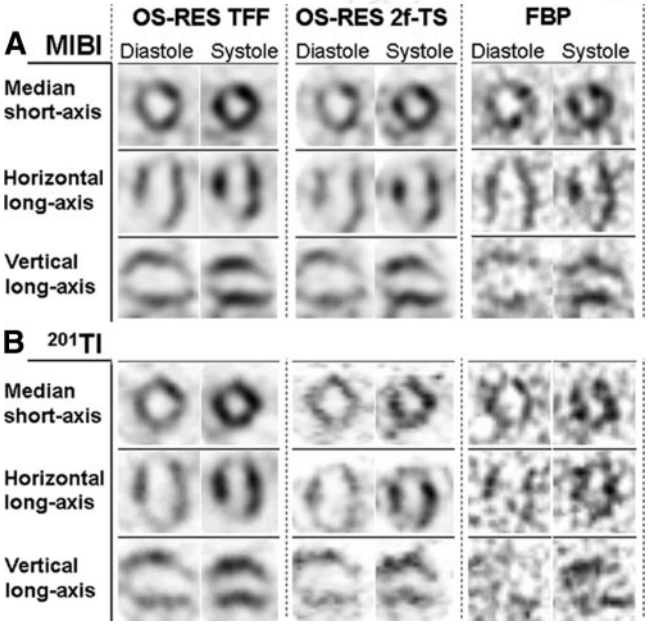

FIGURE 6. Patient with akinetic apical LV area related to previous history of anterior infarction. For sestamibi (MIBI) (A) and, especially, ^{201}Tl (B), image quality is low when reference FBP reconstruction is used (cutoff filter frequency, 0.30 cycles per pixel, with no temporal smoothing). Image interpretation is markedly facilitated and enhanced when the association of OSEM with depth-dependant resolution recovery prefiltering (OS-RES) is combined with 2-frame temporal smoothing (2f-TS) or moreover, with temporal Fourier filtering (TFF).

16- instead of 8-interval gating (*1,2*). As could be expected, the mean number of myocardial counts per interval frame was high enough for sestamibi (650,000) but not for ^{201}Tl (220,000), based on the number of counts (>500,000 (*19*)) required to determine LV ejection fraction with a low vulnerability to noise level. For both tracers, however, dramatic noise reduction and highly accurate assessments of LV function were obtained with the association of OSEM reconstruction with depth-dependant resolution recovery and temporal Fourier filtering.

Ejection fractions were determined with correlation coefficients higher than 0.9, without any underestimation, and this finding agrees with previous observations in 16- but not 8-interval gated SPECT studies (*1,2*). In addition, this determination was clearly better than that from FBP, with lower relative errors and higher correlation coefficients with MRI, even when temporal smoothing was used to lower the noise of FBP images and despite the fact that optimal frequencies of FBP had previously been selected.

The association of OSEM with depth-dependant resolution recovery prefiltering and temporal Fourier filtering also enhanced the visual analysis of segmental contractility: All studies became of sufficient quality to be analyzed visually, and higher κ-values were obtained from visually analyzable reconstructions (Fig. 5). Exact agreement rates with MRI were high for sestamibi (79%) and a little lower for ^{201}Tl (73%). Such high rates had already been reported with tetrofosmin or sestamibi (*20,21*) but not with ^{201}Tl (*21,22*).

By correcting collimator response, the depth-dependant resolution recovery prefilter improves and homogenizes spatial resolution on the overall myocardial volume (*6,11–13*), and the OSEM iterative method presents numerous advantages over FBP, including better noise properties (*3,4*) and the possible incorporation of temporal Fourier filtering at each iteration (*5*). Temporal Fourier filtering consists of a truncating Fourier series of the voxel count variations between interval frames. In this way, SPECT images are obtained at each interval using the activity recorded at all intervals. This process is, therefore, definitely different from that of usual reconstructions, which are performed at each interval on only a small fraction of the recorded activity, especially when 16-interval gating is used.

On the low-count images provided by ^{201}Tl gated SPECT, the association of OSEM with a depth-dependant resolution recovery prefilter has already been shown to substantially improve LV volume determination (*6*). In addition, applying temporal Fourier filtering after OSEM iterations has been found to be associated with introduction of a negligible error but also with a dramatic reduction in noise, corresponding to a more than 2-fold increase in time acquisition (*5*). In agreement with this observation, our study shows that, when associated with OSEM and depth-dependent recovery prefiltering, temporal Fourier filtering improves the signal-to-noise ratio and hence, visual analysis of regional contractility, without any deterioration in the determination of LV volume and ejection fraction. By contrast, determination of LV ejection fraction was affected when strong 3- or 4-frame temporal smoothing was added to depth-dependant resolution recovery reconstructions.

A limitation of the study is that the specific impacts of OSEM, temporal Fourier filtering, and depth-dependant resolution recovery filtering were not analyzed separately. These impacts will require further investigations. However, the intent of this study was to investigate only the likelihood that associations—such as that of OSEM with temporal Fourier filtering and depth-dependant resolution recovery filtering—would reduce the noise of 16-interval gated SPECT images without affecting image resolution. A decrease in image resolution is, indeed, a common disadvantage of usual noise reduction methods (decrease in filter frequency, increase in voxel size, temporal smoothing).

The improvement that was observed between FBP and the association of OSEM with temporal Fourier filtering and depth-dependant resolution recovery filtering was more marked for low image counts and especially for ^{201}Tl image counts. Therefore, this improvement could be less for higher image counts such as those recorded with higher injected activities and longer scanning times. Such longer times, however, increase patients' discomfort and the risk of motion during acquisition, a crucial factor in the reliability of gated SPECT results (*7*). Moreover, further improvements in the signal-to-noise ratio of high-count images might offer the opportunity to use lower voxel sizes at acquisition (zooming, increase in matrix size). According to a previous study (*23*), this option might prevent the LV volume underestimation that has been documented consistently in previous gated SPECT studies (*5,20,24*) and in the present study.

CONCLUSION

This study showed that when gated SPECT acquisitions are recorded with 16-interval gating, the association of OSEM with temporal Fourier filtering and depth-dependant resolution recovery filtering assesses global and regional LV function highly accurately, especially when sestamibi rather than ^{201}Tl is used, and dramatically reduces image noise, a property that is likely to facilitate image interpretation. This association is clearly superior to optimized FBP, whatever the considered tracer and even when the noise of FBP images is reduced by conventional temporal smoothing.

ACKNOWLEDGMENTS

We thank the University Hospital at Nancy for financial and organizational support; Jean-Marc Gravier for help with image analysis; and the staff of SMV-General Electric France, especially François Roche, Dominique Marlier, and Christophe Bravais, for technical support.

REFERENCES

1. Manrique A, Koning R, Cribier A, Vera P. Effect of temporal sampling on evaluation of left ventricular ejection fraction by means of thallium-201 gated SPET: comparison of 16- and 8-interval gating, with reference to equilibrium radionuclide angiography. *Eur J Nucl Med.* 2000;27:694–699.
2. Germano G, Kiat H, Kavanagh PB, et al. Automatic quantification of ejection fraction from gated myocardial perfusion SPECT. *J Nucl Med.* 1995;36:2138–2147.
3. Wilson DW, Tsui BMW. Noise properties of filtered-backprojection and ML-EM reconstructed emission tomographic images. *IEEE Trans Sci.* 1993;40:1198–1203.
4. Barrett HH, Wilson DW, Tsui BMW. Noise properties of the EM algorithm: I. Theory. *Phys Med Biol.* 1994;39:833–846.
5. Vanhove C, Franken PR, Defrise M, Deconinck F, Bossuyt A. Reconstruction of gated myocardial perfusion SPET incorporating temporal information during iterative reconstruction. *Eur J Nucl Med Mol Imaging.* 2002;29:465–472.
6. Daou D, Pointurier I, Coaguila C, et al. Performance of OSEM and depth-dependent resolution recovery algorithms for the evaluation of global left ventricular function in ^{201}Tl gated myocardial perfusion SPECT. *J Nucl Med.* 2003;44:155–162.
7. Djaballah W, Muller MA, Bertrand AC, et al. Gated SPECT assessment of left ventricular function is sensitive to small patient motions and to low rates of triggering errors: a comparison with equilibrium radionuclide angiography. *J Nucl Cardiol.* 2005;12:78–85.
8. Hassan N, Escanye JM, Juilliere Y, et al. ^{201}Tl SPECT abnormalities, documented at rest in dilated cardiomyopathy, are related to a lower than normal myocardial thickness but not to an excess in myocardial wall stress. *J Nucl Med.* 2002;43:451–457.
9. Marie PY, Mertes PM, Hassan-Sebbag N, et al. Exercise release of cardiac natriuretic peptides is markedly enhanced when patients with coronary artery disease are treated medically by beta-blockers. *J Am Coll Cardiol.* 2004 4;43:353–359.
10. Vera P, Manrique A, Pontvianne V, Hitzel A, Koning R, Cribier A. Thallium-gated SPECT in patients with major myocardial infarction: effect of filtering and zooming in comparison with equilibrium radionuclide imaging and left ventriculography. *J Nucl Med.* 1999;40:513–521.
11. Formiconi AR, Pupi A, Passeri A. Compensation of spatial system response in SPECT with conjugate gradient reconstruction technique. *Phys Med Biol.* 1989;34:69–84.

12. Liu L, Cullom SJ, White ML. A modified Weiner filter method for nonstationary resolution recovery with scatter and iterative attenuation correction for cardiac SPECT [abstract]. *J Nucl Med.* 1996;37(suppl):210P.
13. Links JM, Leal JP, Mueller-Gaertner HW, Wagner HN. Improved positron emission tomography quantification by Fourier-based restoration filtering. *Eur J Nucl Med.* 1992;19:925–932.
14. Bacharach SL, Green MV, Vitale D, et al. Optimum Fourier filtering of cardiac data: a minimum-error method—concise communication. *J Nucl Med.* 1983;24: 1176–1184.
15. Germano G. Automatic analysis of ventricular function by nuclear imaging. *Curr Opin Cardiol.* 1998;13:425–429.
16. Cerqueira MD, Weissman NJ, Dilsizian V, et al. Standardized myocardial segmentation and nomenclature for tomographic imaging of the heart: a statement for healthcare professionals from the Cardiac Imaging Committee of the Council on Clinical Cardiology of the American Heart Association. *Circulation.* 2002; 105:539–542.
17. Bluemke DA, Boxermann JL, Atalar E, McVeigh ER. Segmented k-space cine breath-hold cardiovascular MR imaging. I. Principle and technique. *AJR.* 1997; 169:395–400.
18. Li W, Stern JS, Mai VM, Pierchala LN, Edelman RR, Prasad PV. MR assessment of left ventricular function: quantitative comparison of fast imaging employing steady-state acquisition (FIESTA) with fast gradient echo cine technique. *J Magn Reson Imaging.* 2002;16:559–564.
19. Achtert AD, King MA, Dahlberg ST, Pretorius PH, LaCroix KJ, Tsui BM. An investigation of the estimation of ejection fractions and cardiac volumes by a quantitative gated SPECT software package in simulated gated SPECT images. *J Nucl Cardiol.* 1998;5:144–152.
20. Bax JJ, Lamb H, Dibbets P, et al. Comparison of gated single-photon emission computed tomography with magnetic resonance imaging for evaluation of left ventricular function in ischemic cardiomyopathy. *Am J Cardiol.* 2000;86:1299–1305.
21. DePuey EG, Parmett S, Ghesani M, Rozanski A, Nichols K, Salensky H. Comparison of Tc-99m sestamibi and Tl-201 gated perfusion SPECT. *J Nucl Cardiol.* 1999;6:278–285.
22. Cwajg E, Cwajg J, Keng F, He ZX, Nagueh S, Verani MS. Comparison of global and regional left ventricular function assessed by gated SPECT and 2-D echocardiography. *Rev Port Cardiol.* 2000;19(suppl 1):I39–I46.
23. Nakajima K, Taki J, Higuchi T, et al. Gated SPET quantification of small hearts: mathematical simulation and clinical application. *Eur J Nucl Med.* 2000;27: 1372–1379.
24. Yoshioka J, Hasegawa S, Yamaguchi H, et al. Left ventricular volumes and ejection fraction calculated from quantitative electrocardiographic-gated ^{99m}Tc-tetrofosmin myocardial SPECT. *J Nucl Med.* 1999;40:1693–1698.

snm
advancing molecular imaging